Int. J. Electrochem. Sci., 13 **(2018)** 9803 – 9815, doi: 10.20964/2018.10.59

International Journal of
ELECTROCHEMICAL
SCIENCE
www.electrochemsci.org

Synergistic Effects between Gemini Inhibitor and Thiourea/thiazole/pyridine as Corrosion Inhibitors on N80 Steel in Brine Solution with Saturated CO_2

Fuqiang Hu[1], *Weiqiang Zhang*[1], *Jun Tang*[2], *Juan Xie*[2], *Junlei Tang*[3], *Jianpeng Mao*[4], *Hu Wang*[2,*]

[1] CNOOC Changzhou EP Coating Co. Ltd., Changzhou 213016, China, China
[2] School of Materials Science and Engineering, Southwest Petroleum University, Chengdu 610500, China
[3] College of Chemistry and Chemical Engineering, Southwest Petroleum University, Chengdu 610500, China
[4] Beijing BSS Corrosion Protection Industry Co., Ltd., Beijing 100029, China
[*]E-mail: senty78@126.com

Received: 22 May 2018 / *Accepted:* 20 July 2018 / *Published:* 1 September 2018

Inhibition performances of gemini imidazoline inhibitor on N80 steel in a CO_2-saturated brine solution have been researched using weight loss and electrochemical methods. The synergistic effects of gemini with other inhibitors have also carried out with chemical and electrochemical measurements. It is shown that the gemini inhibitor can inhibit corrosion effectively. Gemini inhibitor is anodic type. Gemini and other inhibitors exists apparent synergistic effect. The mixed inhibitors demonstrate excellent protection to N80 steel. The best formula of mixture inhibitors is presented, 10 mg/L gemini + 2 mg/L thiourea (TU) + 5 mg/L thiazole (TZ) + 5 mg/L pyridine (PD). The synergistic mechanism of gemini with other inhibitors is also proposed.

Keywords: N80 steel, polarization curve, EIS, gemini corrosion inhibitor

1. INTRODUCTION

Corrosion extensively exists in most processes of oil and natural gas production [1-4]. Many factors have remarkable effects on the corrosion of carbon steel used in such environment, like water content, partial pressure of gases, temperature, flow rate of fluids, solid particles, the presence of bacteria, salinity, presence and concentration of carbon dioxide and hydrogen sulfide, materials condition, and so on [5-9]. Therefore, it is a rather complex process for corrosion in petroleum exploitation.

Carbon dioxide exists in most of the wells. It plays an influence on the corrosion of produced liquid. The dissolution of carbon dioxide usually decreases the pH value of the system. Therefore the anodic process of corrosion is often the hydrogen depolarization. In addition, at high temperature and pressure, carbon dioxide is commonly in a supercritical state, in which the corrosion process gets more complicated [10-12]. Severe acidic corrosion often occurred at tubing string, valves of wellhead, oilfield ground system and re-injection system [13, 14].

Although higher grade of materials are often applied in practice [15, 16], adding corrosion inhibitor still remains the most useful and economic measure to alleviate corrosion in most circumstances. In industrial applications, organic molecules with N, O, S and P groups are usually used as main ingredients of commercial corrosion inhibitors. Such groups are commonly excellent electron donor and can provide strong bonding between organic molecule and metal at interface [17, 18]. Such bonding not only can enhance the chemical stability of metal surface, but also can form a barrier between metal matrix and aggressive medium.

In practical application, mixtures of different chemicals with imidazoline are commonly used, not only for better performance but also for economic consideration. The synergistic effect between imidazoline and other chemicals has also been widely investigated [19-25]. Jingmao Zhao et al. [19] studied the synergistic effect of imidazoline and sodium benzoate at mild steel surface in near neutral environment. Experiment results show that sodium benzoate observably improve the inhibition efficiency of imidazoline. Imidazoline and sodium benzoate exist obviously synergism. A model was also presented to explain the mechanism of synergism. Thiourea (TU) is an important chemical in the formulation of corrosion inhibitor. While it has a relatively narrow dosage in acidic condition, otherwise it will speed up corrosion process. P. C. Okafor et al. [20] found that obviously synergistic effect existed between 2M2 and TU on N80 steel in CO_2 solutions. It is shown that adding of 2M2 enhanced the adsorption of TU. The compounds retard the corrosion reactions via their polycentric adsorption sites on N80 surface. Adsorption of 2M2 meets with Langmuir adsorption isotherm. Numerous synergism studies in regard to imidazolines and halides had been widely reported [21-25]. The synergistic effect between imidazoline and iodine ions for galvanic corrosion was studied by M. Heydari and M. Javidi [21]. It was proved that I^- can change the distribution of excess charge on galvanic electrode, which enhances the adsorption of imidazoline on both electrodes. P. C. Okafor et, al. [22] also proved the synergism between imidazoline and iodine ion in acidic media. The presence of I^- increased the inhibition efficiency of imidazoline. The unpolarization potentials were observed in the presence of potassium iodide and it increased with the concentration. However, most of the previous works focused on the synergistic effect of imidazoline and another chemical, usually halides or thiourea. In practice, the formulation of corrosion inhibitor is often consisted of more than three chemicals. More work should be done in synergism of three or more chemicals.

In this paper, the inhibition efficiency of gemini imidazoline inhibitor on N80 steel has been studied in a CO_2-saturated brine solution at 70℃ by weight loss and electrochemical methods. In addition, the synergism of gemini imidazoline inhibitor with other inhibitors are also studied with weight loss and electrochemical measurements.

2. EXPERIMENTAL

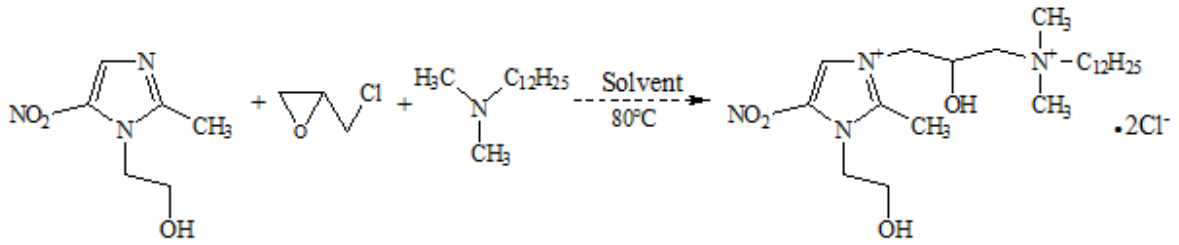

Figure 1. The synthetic reaction and chemical structure of the gemini inhibitor.

The gemini corrosion inhibitor was synthesized and purified in lab. The synthetic reaction and structural formula of the inhibitor is shown in Fig. 1. It is shown that it has the imidazoline structure and belongs to gemini type in nature. In addition, the inhibitor behaves asymmetrical structure. Thiourea (TU), thiazole (TZ) and pyridine (PD) were used as inhibitors for synergistic experiments.

The test corrosion medium was composed of 1.265 g/L $CaCl_2$, 0.148 g/L Na_2SO_4, 2.896 g/L NaCl, 0.556 g/L KCl, 1.309 g/L $MgCl_2 \cdot 6H_2O$, 0.497 g/L $NaHCO_3$ and 0.056 g/L $NaCO_3$, which represents the composition of the produced water of an south China offshore oilfield. De-ionized water was used for solution preparation. And all the reagents used in the experiments are analytical grade. The experiments were carried out at 70℃, which is the temperature of production system.

N80 steel was used as experimental material with the chemical composition (wt) of C (0.395%), Si (0.242%), Mn (1.400%), P (0.017%), S (0.004%), Cr (0.063%), Ni (0.071%), Mo (0.025%), Cu (0.114%), V (0.110%) and Fe (remainder). Rectangular specimens with surface areas of 1000 mm^2 were used in weight loss measurements. In electrochemical experiments, the rectangular specimens were embedded with epoxy resin, leaving an area of 10 mm × 10 mm exposed to the electrolyte. All specimens were abraded carefully with silicon carbide paper gradually from 800 up to 2000 grits, rinsed with de-ionized water, ethanol, acetone, and dried in cold air before experiments.

In weight loss tests, the specimens were immersed into the prepared solution for 72 hours in static condition. The corrosion medium was deaerated and saturated with CO_2 beforehand. After experiments, the corrosion products were wiped off by cleaning solution (10% HCl + 1% Urotropine) and then the corrosion rate was calculated as the following equation:

$$\eta = \frac{r_0 - r}{r_0} \times 100\% \qquad (1)$$

where η stands for inhibition efficiency. r_0 and r are the corrosion rates in the absence and presence of corrosion inhibitor, respectively. Three specimens were used in each measurement.

The electrochemical measurements were conducted by Iviumstat Electrochemical Interface (Iviumtechnologies, Netherlands). The electrolytic cell was filled with 250 ml solution. The corrosion medium was deaerated with N_2 and saturated with CO_2 before electrochemical test. The reference electrode was the saturated calomel electrode (SCE) and platinum bar was served as counter electrode. The working electrode was the finely polished N80 steel. It had been immersed in the test solution for 1 h to monitor the open circuit potential (OCP) before every electrochemical measurements. In polarization curve measurements (PC), the scanning operation was carried out from -0.250 V (vs.

OCP) to +0.250 V (vs. OCP) with a scanning rate of 0.3 mV/s. η was calculated as following expression:

$$\eta = \frac{I_{corr(0)} - I_{corr(1)}}{I_{corr(0)}} \times 100\% \quad (2)$$

where $I_{corr(0)}$ and $I_{corr(1)}$ are corrosion current densities in the absence and presence of corrosion inhibitor. In electrochemical impedance spectroscopy measurement (EIS), the amplitude of the applied alternative current was ±10 lmV. All the EIS tests were proceeded at OCP. The range of frequency for EIS was from 10^5 Hz to 10^{-2} Hz. Inhibition efficiency for EIS measurements were obtained by the following equation:

$$\eta = \frac{R_p' - R_p}{R_p'} \times 100\% \quad (3)$$

where R_p' and R_p are the charge transfer resistance (Ω cm^2) in the presence and absence of corrosion inhibitor, respectively.

The surface morphologies after different weight loss tests were compared by scanning electronic microscopy (SEM, EVO MA 15, Zeiss Nano Techno.).

3. RESULTS AND DISCSSION

3.1 Weight loss measurements

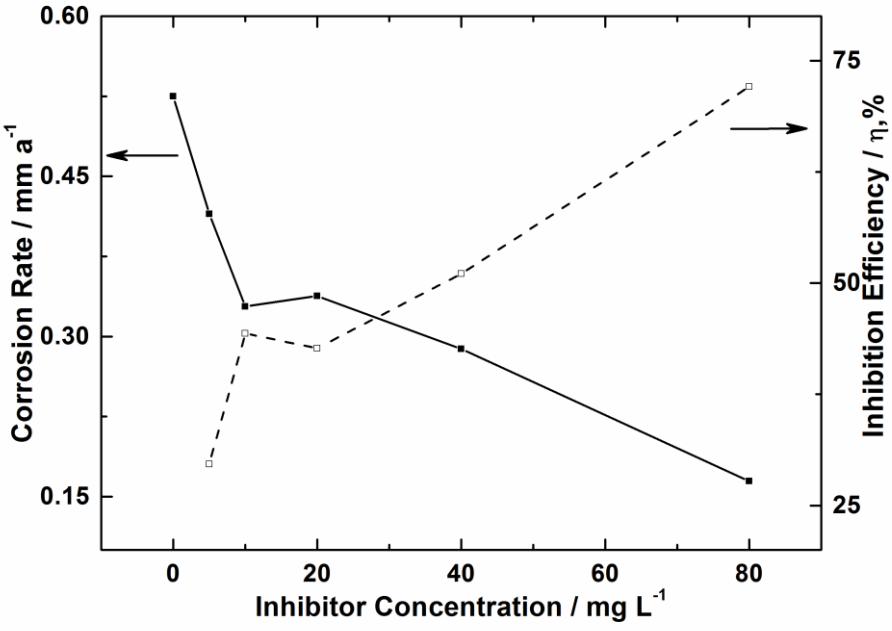

Figure 2. Weight loss measurements of gemini inhibitor on N80 steel in a CO_2-saturated brine solution in static experiments at 70℃.

Fig. 2 shows the variations of corrosion rate and inhibition efficiency (η) of gemini inhibitor on N80 steel in a CO_2-saturated brine solution in static experiments at 70℃ with concentrations. It is

shown that the corrosion rates remarkably decrease and η increase with the presence and increase of inhibitor. It also shows the higher the inhibitor concentration, the lower corrosion rates and the higher η, which indicates that the inhibitor is highly efficient in high concentration.

Several adsorption isotherms were used to fit the obtained data. Langmuir adsorption isotherm fits the best for the Gemini inhibitor, which accords the following expressions:

$$\frac{C_{inh}}{\theta} = \frac{1}{K} + C_{inh} \quad (4)$$

$$K = \frac{1}{55.5}\exp(-\frac{\Delta G_{ads}^{0}}{RT}) \quad (5)$$

where C_{inh} is the inhibitor concentration, θ stands for the surface coverage, K is the adsorptive equilibrium constant, ΔG_{ads}^{0} represents the standard free energy of adsorption, R and T are the gas constant and the temperature of measurement , respectively[26, 27].

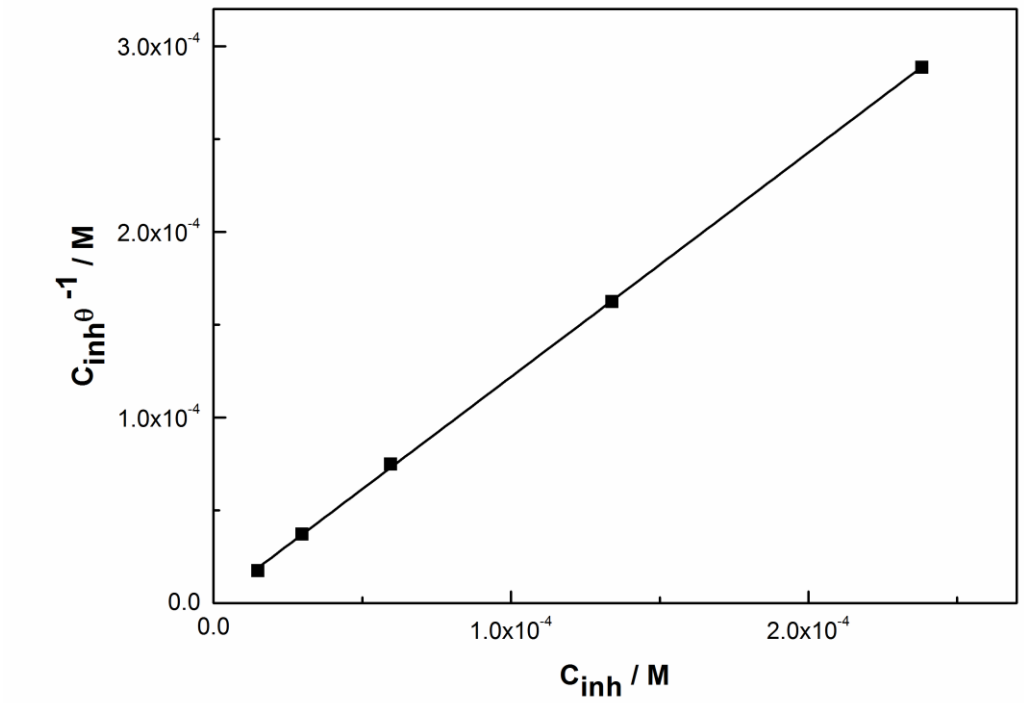

Figure 3. Langmuir adsorption of gemini inhibitor on N80 steel in a CO_2-saturated brine solution at 70℃.

Fig. 3 demonstrates the relationship of C/θ and C without and with different concentrations of gemini inhibitor. The linear regression coefficient is over 0.99, which implies the adsorption process fits Langmuir adsorption well. The ΔG_{ads}^{0} for the inhibitor is -28.5 kJ mol^{-1}. It is generally assumed that the negative value of ΔG_{ads}^{0} indicates a spontaneous adsorption of gemini inhibitors at the metal surface [28, 29]. ΔG_{ads}^{0} value less than -40 kJ mol^{-1} indicates charge sharing or transfer from the inhibitor molecules to metal surface, which indicates a chemical adsorption process in nature. While values more than -20 kJ mol^{-1} are assumed as physical adsorption [22]. In our study, the value of

ΔG_{ads}^{0} of adsorption is between the range and closer to -20 kJ mol^{-1}. Hence, physical adsorption is dominated for gemini inhibitor on the metal surface.

3.2 Electrochemical behavior of gemini inhibitor

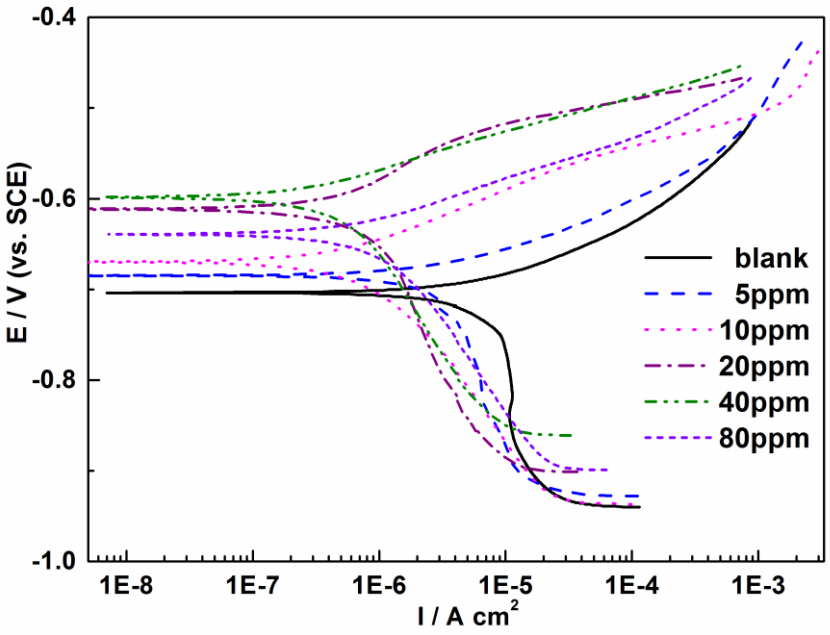

Figure 4. Polarization curves of N80 without and with gemini inhibitor in a CO_2-saturated brine solution at 70℃.

In order to understand the inhibition mechanism of gemini inhibitor, electrochemical measurements, including polarization curves and EIS were performed in simulated solution at 70℃. Fig. 4 presents the polarization curves of gemini inhibitor in different concentrations. And Table 1 shows the relevant electrochemical parameters fitted from polarization curves, corrosion potential (E_{corr}), Tafel constants (b_a and b_c), corrosion current density (I_{corr}) and η included.

Table 1. Electrochemical parameters from polarization curves of N80 steel without and with three gemini inhibitors in a CO_2-saturated brine solution at 70℃.

Conc. / mgL^{-1}	E_{corr} / V	$I_{cor}/10^{-7}$ A cm^{-2}	b_a / mV dec^{-1}	$-b_c$ / mV dec^{-1}	η / %
blank	-0.704	98.5	192	1201	-
5	-0.686	33.0	57	517	66.5
10	-0.671	9.92	135	209	89.9
20	-0.671	9.60	130	206	90.3
40	-0.597	4.59	67	222	95.3
80	-0.638	8.69	62	192	91.2

Fig. 4 presents that the presence of gemini inhibitor notably affects the polarization curves. All the polarization curves exhibit typical active dissolution in anode. The presence of any of the inhibitor causes apparent change in position and shape of the polarization curve. The corrosion current density falls with the increase of inhibitor concentration, indicating this inhibitor is very efficient in retarding corrosion of N80 steel. η variations also prove the high efficiency, shown in Table 1. η values can be higher than 85% at high concentrations, especially it reaches to 95.3% in the concentration of 40 mg/L. The presence of corrosion inhibitor also shifts the corrosion potential E_{corr} to positively, revealing that the inhibitor has more remarkable influence on the anodic reaction than the cathodic reaction. In literature, it is reported that if the shifting in E_{corr} is more than 85 mV, the inhibitor can be classified as a cathodic or anodic type [30]. In our study, the maximum shifting of E_{corr} value is less than 85 mV towards anodic region. While it is obvious in polarization curves that the cathodic reactions are of the same order of magnitude, showing relatively little inhibition, but the anodic reaction is severely inhibited. It can be concluded that it is mainly the anodic reaction prevailing.

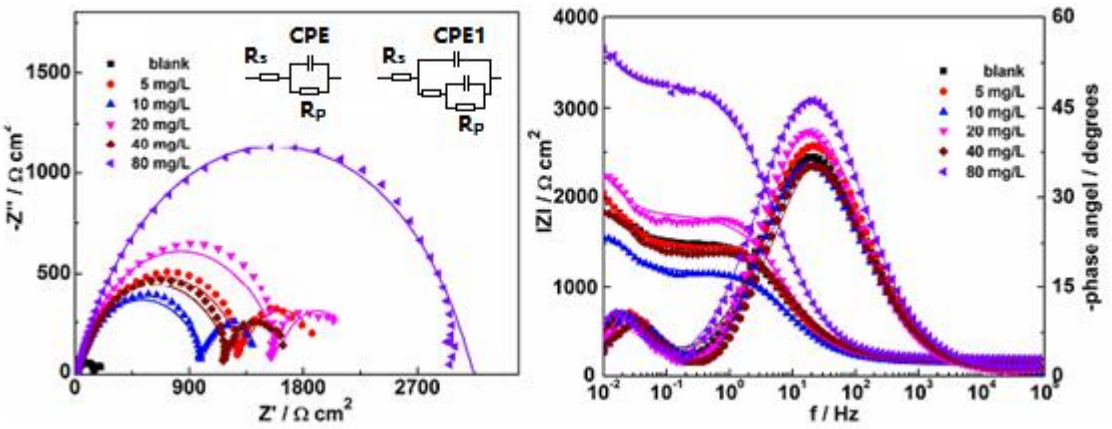

Figure 5. EIS plots of N80without and with gemini inhibitor in a CO_2-saturated brine solution at 70℃.

The inhibition behavior of gemini inhibitor with various concentrations on N80 steel was investigated by EIS measurements. The influence of inhibitor concentration on impedance spectrum is presented in Fig. 5 with Nyquist and Bode plots. The impedance keeps rising with inhibitor concentration. All of the Nyquist plots exhibit depressed capacitive semicircular in all frequency range, which is because of the charge transfer reaction and the roughness and inhomogeneities of the metal surface [31-33]. The EIS plot in the absence of corrosion inhibitor contains only one capacitive loop, indicating only one electrochemical kinetic process at the interface. It also proves corrosion reaction of N80 steel in CO_2 solution is primarily controlled by charge transfer process. While in the presence of gemini corrosion inhibitor, the appearance of the plots changes remarkably. It is shown that in the presence of gemini inhibitor, two capacitive loops can be seen from Nyquist plot. The one at higher frequency corresponds to the polarization resistance at the interface. The diameter increased with the adding of inhibitor and also rose with the concentration of inhibitor. In the presence of 80 mg/L inhibitor, only one capacitive loop exists. The diameter of the loop is the biggest in all, indicating the best performance of adsorption film at the interface.

It also can be observed from the Bode plots that the shape in blank solution differs from the one with the presence gemini inhibitor. Typical electrical equivalent circuit can be involved to explain the impedance in the absence and presence of gemini inhibitor. It presents two capacitive loops condition, absence and presence of gemini inhibitor. From the equivalent circuit, R_s represents the electrolyte resistance (Ω cm^2), R_p stands for the charge transfer resistance (Ω cm^2) and a constant phase element CPE (Ω^{-1} s^n cm^2) is used instead of an ideal capacitor. The CPE is expressed as follows:

$$\mathrm{CPE} = \frac{1}{Q} \times \frac{1}{(j\omega)^n} \quad (6)$$

where Q represents the CPE coefficient, ω is $2\pi f$, n means the phase shift and j stands for the imaginary unit. Table 2 shows all the parameters of EIS of the gemini inhibitors. η values of all conditions were calculated by using R_p according to equation (3). It is shown that the inhibitor presents excellent η, especially at high concentration, which accords the results of weight loss and polarization curve measurements.

Table 2. Electrochemical parameters obtained from fitting of EIS, on N80 steel in the absence and presence of gemini inhibitor in a CO_2-saturated brine solution at 70℃.

Conc. / mgL^{-1}	R_p / Ω cm^2	CPE/$\mu\Omega^{-1}$ s^n cm^2	n	η / %
blank	62	469	0.78	0
5	588	401	0.79	89.5
10	432	526	0.78	85.6
20	585	336	0.82	89.4
40	464	369	0.79	86.6
80	3087	64	0.82	98.0

3.3 Synergism of gemini inhibitor with other inhibitors

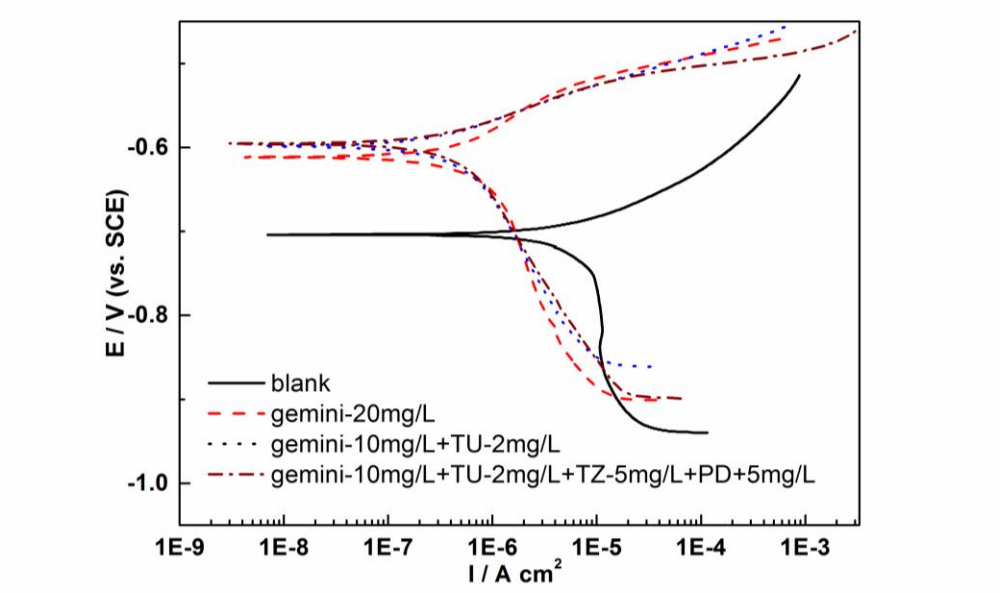

Figure 6. Potentiodynamic polarization curves of gemini inhibitor formulated with other inhibitors on N80 steel in a CO_2-saturated brine solution in static experiments at 70℃.

Electrochemical measurements were performed to explain the synergistic effects of gemini and other inhibitors. Fig. 6 shows synergistic effects in polarization curve results of gemini inhibitor with other inhibitors and Table 3 shows the electrochemical parameters obtained from Fig. 6. It is shown that both b_a and b_c considerably decreases with the presence of the mixture inhibitors, indicating the mixture inhibitors inhibit the both cathodic and anodic process. Meantime, E_{corr} moves positively when adding corrosion inhibitors. As mentioned above, the displacement of E_{corr} is less than 85mV in all concentrations for gemini inhibitors, indicating that the gemini are mixed type inhibitor. In the presence of 10 mg/L gemini + 2 mg/L TU and 10 mg/L gemini + 2 mg/L TU + 5 mg/L TZ + 5 mg/L PD, displacements of E_{corr} towards positive direction are over 100 mV. It is obvious that the mixed inhibitors are anodic type corrosion inhibitors. This result suggests that the mixed inhibitors retard the corrosion of steel by inhibiting the anode process of corrosion.

Table 3. Electrochemical parameters from polarization curves of N80 steel in the absence and presence of formulated inhibitors in a CO_2-saturated brine solution at 70°C.

Concentration	E_{corr}/V	I_{cor} /10^{-7} A cm^{-2}	b_a / mV dec^{-1}	-b_c / mV dec^{-1}	η / %
blank	-0.7042	98.5	192	1201	-
20 mg/L gemini	-0.6708	9.60	130	206	90.3
10 mg/L gemini + 2 mg/L TU	-0.5903	4.80	74	223	95.1
10 mg/L gemini + 2 mg/L TU + 5 mg/L TZ + 5 mg/L PD	-0.6007	4.41	70	111	95.5

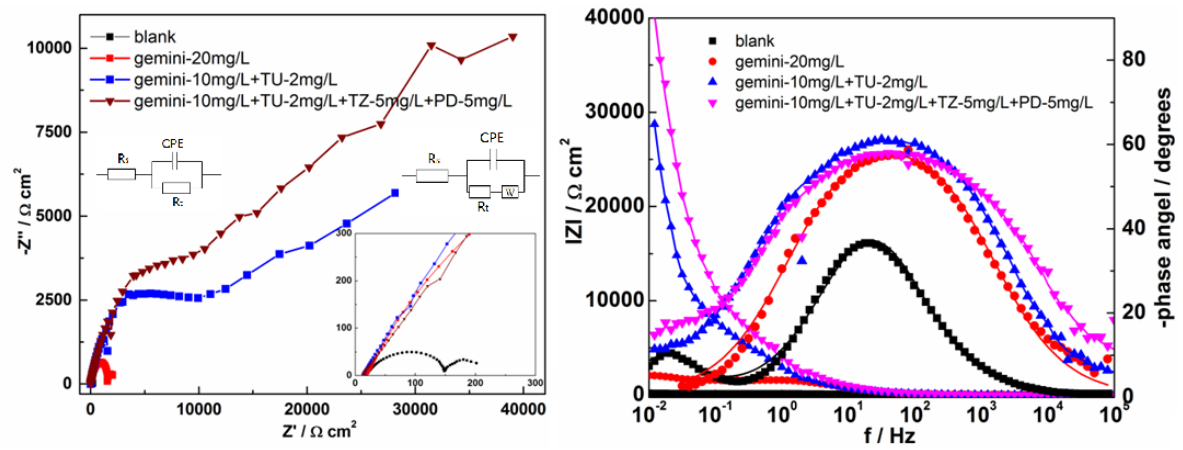

Figure 7. Nyquist and Bode plots of gemini inhibitor formulated with other inhibitors on N80 steel in a CO_2-saturated brine solution in static experiments at 70°C.

Fig. 7 shows the Nyquist and Bode plots of N80 steel in the presence of different corrosion inhibitors. Distinct Warburg impedance appears at low frequency region in the presence of gemini inhibitor + TU and gemini inhibitor + TU + TZ + PD, which can be observed from Nyquist plots of gemini inhibitor. The presence of Warburg impedance reveals the mass transport in nature. The slope

of diffusion tail is less than 45°. It could be ascribed to the porous inhibitor film developed on the N80 surface. The diffusion impedance element demonstrates the electrochemical process is controlled by diffusion process, in which the aggressive ion, like chloride ion, usually diffuses and adsorbs at the metal surface or corrosion products diffuse away from the metal surface through the inhibitor film to the bulk solution. Such process is the slowest process in all electrochemical processes. And it becomes the control step. All measurements have shown in Nyquist plots that there is only one capacitive loop in medium frequency region. It is always believed that the higher the R_p, the better the protective film existed on metal surface. And η of corrosion inhibitor can also be calculated from R_p. All electrochemical parameters from EIS are shown in Table 4. It is shown that the presence of TU and other chemicals enlarges R_p greatly. Hence, η increases high up to more than 95%. The N80 surface can be well protected by all the mixture corrosion inhibitors.

Table 4. Electrochemical parameters from EIS measurements of N80 steel in the absence and presence of formulated inhibitor in a CO_2-saturated brine solution at 70℃.

Inhibitors	CPE /10^{-6} s^n Ω^{-1} cm^{-2}	n	R_p / Ω cm^2	W / 10^{-4} Ω cm^2	η / %
blank	469	0.78	62	-	-
20 mg/L gemini	369	0.79	464	-	89.4
10 mg/L gemini + 2 mg/L TU	7.45	0.71	13920	6.99	97.5
10 mg/L gemini + 2 mg/L TU + 5 mg/L TZ + 5 mg/L PD	62.9	0.66	28090	9.20	98.7

3.4 Surface morphological examination

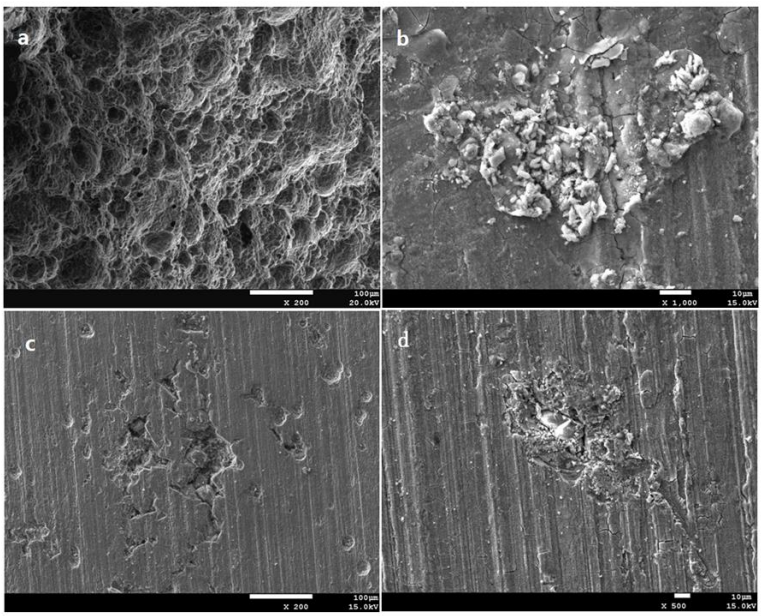

Figure 8. SEM images for N80 steel (a) in the absence of inhibitor; (b) in the presence of 20mg/L gemini inhibitor; (c) in the presence of 20mg/L gemini + 2mg/L TU; (d) N80 steel with 20mg/L gemini + 2mg/L TU+5 mg/L TZ+ 5 mg/L PD.

Surface morphologies of N80 steel surface, without and with different inhibitors obtained from weight loss experiments at 70℃ for 72 h , were examined in SEM. The difference between specimens is apparent, unprotected specimen exhibits very rough surface after cleaning the corrosion products, shown in Fig. 8a. Fig. 8b is the image of N80 in the presence of 20 mg/L gemini inhibitor. It is shown that the surface is partly protected by inhibitor. While apparent corrosion still can be observed. In Fig.c and Fig.d, the specimens are only slightly corroded. The N80 steels is well protected by mixture inhibitor of gemini + TU + TZ + PD. It demonstrates that the mixture inhibitor has excellent inhibition efficiency on N80 steel in studied condition.

3.5 The mechanism of gemini inhibitor

The inhibition mechanism of imidazoline has been thoroughly investigated. It is generally believed that imidazoline molecule adsorbs on metal surface with the hydrophilic group of imidazoline ring, which is excellent electron donor. Meantime, the hydrophobic alkyl chain, forming hydrophobic arrays, stretches into the water to prevent the invasion of aggressive ions in solution, like chloride ion. Monolayer and double layer adsorptions were both proposed and this may be determined by different imidazoline molecular structures. In our study, gemini inhibitor is cationic gemini surfactant and contains imidazoline structure, meaning that at least containing two hydrophilic groups in the molecule. And the adsorption process of inhibitors can be enhanced. The existence of -OH and $-NO_2$ in gemini inhibitor structure enhances the solubility of the inhibitor and alkyl chain–$C_{12}H_{25}$ repels the water off the interface. However, the asymmetric structure impedes the gemini inhibitor to adsorb on metal surface with high coverage from stereo-hindrance viewpoint. In addition, only one hydrophobic long chain in structure also hampers the formation of the compact water-resistance layer upon the interface.

When other inhibitors added to the solution, the synergistic effect between gemini inhibitor and other species will occur. The vacancy and uncoated area left by gemini inhibitor will be occupied by TU, TZ and PD. The synergistic effect enhances the coverage of inhibitors on N80 surface. Therefore, after adding mixture inhibitors, corrosion rate decreases and η rises remarkably, both in weight loss or electrochemical measurements.

4. CONCLUSIONS

The inhibition of gemini imidazoline inhibitor on N80 steel was studied using weight loss and electrochemical methods. The synergistic effects between gemini inhibitor and other inhibitors were also investigated. The following conclusions are obtained.

(1) Weight loss, polarization curve and EIS all proved that the gemini inhibitor has pronounced inhibiting properties in corrosion of N80 steel in produced water. The concentration of inhibitor has remarkable influence on the inhibition efficiencies.

(2) The adsorption of gemini corrosion inhibitor obeys Langmuir adsorption. The value of free energy (ΔG_{ads}^0) of adsorption for gemin inhibitor is -28.5 kJ mol^{-1}, suggesting a mixed type adsorption but primarily physical adsorption.

(3) Polarization curves indicate that the gemini inhibitor is anodic corrosion inhibitor, which inhibits anodic dissolution process.

(4) Experiment results show that gemini and other inhibitors exist apparent synergistic effect. The mixture inhibitors provide excellent protection to N80 steel. The best formula of mixture inhibitors is 10 mg/L gemini + 2 mg/L TU + 5 mg/L TZ + 5 mg/L PD. The synergism between gemini and these chemicals reduces the corrosion rate of N80 and increases the inhibition efficiency remarkably. All the mixture inhibitors are anodic corrosion inhibitors. The mixed inhibitors retard the corrosion of steel by inhibiting the anode process of corrosion.

(5) The inhibition mechanism of gemini inhibitor is determined by the detailed structure. The imidazoline ring and other hydrophilic groups enhance the adsorption and alkyl chain ensures the water-resistance layer. The vacancy and uncoated area left by gemini inhibitor at metal surface can be occupied by TU, TZ and PD. The synergistic effect enhances the coverage of inhibitors on N80 surface.

ACKNOWLEDGEMENTS

We are grateful to the supports of National Science Foundation of China (No. 51641108) and the Sichuan Key Lab of Oilfield Materials (No. X151517KCL32).

References

1. M. B. Kermani, A. Morshed, *Corrosion,* 59 (2003) 659.
2. J. Zhang, J. Wang, F. M. Zhu, M. Du, *Ind. Eng. Chem. Res.,* 54 (2015) 5197.
3. H. Wang,Y.S. Liu, J. Xie, J.L. Tang, M. Duan, Y.Y. Wang, M. Chamas, *Int. J. Electrochem. Sci.*, 11 (2016) 4943.
4. R. Case, *Corrosion,* 70 (2014) 1080.
5. X. S. Huang, Y. M. Qi, C. F. Chen, H. B. Yu, G. W. Lu, *Corros. Eng. Sci. Techn.,* 50 (2015) 169.
6. T. Hong, Y. H. Sun, W. P. Jepson, *Corros. Sci.,* 44 (2002) 101.
7. D. A. López, W. H. Schreiner, S. R. de Sánchez, S. Simison, *Appl. Surf. Sci.,* 207 (2003) 69.
8. C.-O. A. Olsson, D. Landolt, *Electrochim. Acta,* 48 (2003) 1093.
9. J. K. Heuer, J. F. Stubbins, *Corros. Sci.,* 41 (1999) 1231-1243.
10. J. Tang, H. Wang, X.Q. Jiang, Z.H. Zhu, J. Xie, J.L. Tang, Y.Y. Wang, M. Chamas, Y. Q, Zhu, H.G. Tian, *Int. J. Electrochem. Sci.,* 13 (2018) 3625.
11. B. R. Linter, G. T. Burstein, *Corros. Sci.,* 41 (1999) 117.
12. D. M. Ortega-Toledo, J. G. Gonzalez-Rodriguez, M. Casales, L. Martinez, A. Martinez-Villafañe, *Corros. Sci.*, 53 (2011) 3780.
13. H. Wang, J. Tang, J. Xie, *Int. J. Electrochem. Sci.,* 12 (2017) 11017.
14. L. S. Moiseeva, *Prot. Met.,* 41 (2005) 76.
15. A. Ikeda, S. Mukai, M. Ueda, *Corrosion,* 41 (1985) 185.
16. L. J. Mu, W. Z. Zhao, *Corros. Sci.,* 52 (2010) 82.
17. M. A. Quraishi, I. Ahamad, A. K. Singh, S. K. Shukla, V. Singh, *Mater. Chem. Phys.,* 112 (2008) 1035.
18. E. A. Flores, O. Olivares, N. V. Likhanova, M. A. Domínguez-Aguilar, N. Nava, D. Guzman-Lucero, M. Corrales, *Corros. Sci.,* 53 (2011) 3899.
19. J. Zhao, G. Chen, *Electrochim. Acta,* 69 (2012) 247.
20. P. C. Okafor, C. B. Liu, X. Liu, Y. G. Zheng, F. Wang, C. Y. Liu, F. Wang, *J. Solid State Electrochem.,* 14 (2010) 1367.
21. 21 M. Heydari, M. Javidi, *Corros. Sci.,* 61 (2012) 148.

22. P. C. Okafor, Y. G. Zheng, *Corros. Sci.*, 51 (2009) 850.
23. P. C. Okafor, C. B. Liu, X. Liu, and Y. G. Zheng, *J. Appl. Electrochem.*, 39 (2009) 2535.
24. J. Zhang, X. L. Gong, H. H. Yu, M. Du, *Corros. Sci.*, 53 (2011) 3324.
25. S. Q. Hu, A. L. Guo, Y. F. Geng, X. L. Jia, S. Q. Sun, J. Zhang, *Mater. Chem. Phys.*, 134 (2012) 54.
26. M. V. Fiori-Bimbi, P. E. Alvarez, H. Vaca, C. A. Gervasi, *Corros. Sci.*, 92 (2015) 192.
27. S. A. Ali, H. A. Al-Muallem, S. U. Rahman, M. T. Saeed, *Corros. Sci.*, 50 (2008) 3070.
28. W. H. Li, Q. He, S. T. Zhang, C. L. Pei, B. R. Hou, *J. Appl. Electrochem.*, 38 (2008) 289.
29. S. Vishwanatham, N. Haldar, *Corros. Sci.*, 50 (2008) 2999.
30. E. S. Ferreira, C. Giancomelli, F. C. Giacomelli, A. Spinelli, Mater. Chem. Phys., 83 (2004) 129.
31. X. H. Li, S. D. Deng, G. N. Mu, H. Fu, F. Z. Yang, *Corros. Sci.*, 50 (2008) 420.
32. H. H. Zhang, X. L. Pang, M. Zhou, C. Liu, L. Wei, K. W. Gao, *Appl. Surf. Sci.*, 356 (2015) 63.
33. J. Cruz, R. Martínez , J. Genesca, E. García-Ochoa, *J. Electroanal. Chem.*, 566 (2004) 111.